Acta Montanistica Slovaca
ISSN 1335-1788
actamont.tuke.sk

Research And Analysis Of Models Of The Moon's Gravity Field

Oksana SERANT[1], Yurii LUKIANCHENKO[2], Ihor ROMANYSZYN[3], Yuliia USHCHUK[1], Nataliya YAREMA[4] and Ostap-Mykhailo SERANT[1]

Authors' affiliations and addresses:
[1] Department of Higher Geodesy and Astronomy, National University Lviv Polytechnic, Ukraine, e-mail: oksana.v.serant@lpnu.ua, juliauschuk@gmail.com, ostap-mykhailo.v.serant@lpnu.ua

[2] Department of Economic Expertise and Land Management, West Ukrainian National University, Ukraine, e-mail: y.lukyanchenko@wunu.edu.ua

[3] Department of Geodesy and Geomatics, Kielce University of Technology, Poland, e-mail: iromanyshyn@tu.kielce.pl

[4] Department of Cartography and Geospatial Modelling, National University Lviv Polytechnic, Ukraine, e-mail: nataliia.p.yarema@lpnu.ua

***Correspondence:**
Ihor Romanyszyn, al. Tysiąclecia Państwa Polskiego 7, 25-314, Kielce, Poland, tel.: +48 41 34 24 559
e-mail: iromanyshyn@tu.kielce.pl

How to cite this article:
Serant, O., Lukianchenko, Y., Romanyszyn, I., Ushchuk, Y., Yarema, N., Serant, O.-M. (2026). Research And Analysis Of Models Of The Moon's Gravity Field, *Acta Montanistica Slovaca,* Volume 31 (1), 181-197

DOI:
https://doi.org/10.46544/AMS.v31i1.14

Abstract
The aim of this paper is to analyze the development of models of the Moon's gravitational field by selecting one model each for the specific time interval of the study of the Moon. To compare them and show the difference with already existing models, as well as to generalize and structure the information about the studied models of the gravitational field of the Moon.
To perform the study, input data were obtained from the International Centre for Earth Gravitational Field Models (Ince, E. S. et al., 2019).
The features of the models GLGM-2 (1995), JGL150Q1 (2000), GRGM660PRIM (2013), STU_MoonTopo720_plusNormalField (2019), and AIUB GRAILV-VGRL 350A (2021) under study are analyzed and described.
Two functionals of the geopotential were used in the study: gravitation and height anomaly. Visualization and data processing were performed using the GMT software package (Wessel, P., et al., 2013). Model analysis was performed by comparing and examining the constructed geopotential functional maps.
Maps for the calculated differences for these functionals were constructed, on which the features of the comparative models are clearly visible. Hypotheses explaining the peculiarities found in each of the models under study were presented.
Formulated recommendations for the use of these models in future studies.
Bringing together information on the new models will give scientists a better understanding of the characteristics of a particular model. This will enable a faster and more effective selection of a model for a particular study, facilitating further development and new research for other scientists.

Keywords
Relief of the Moon, models of the Moon's gravity field, height anomaly, mass concentration (mascon), functionals.

Introduction

It is a known fact that the Moon is the only natural satellite of Earth. It is the closest celestial body to our planet (average distance to the Moon is about 384,400 km), and it is the fifth-largest satellite of the solar system.

Fig. 1 presents an image of the Moon captured by the Wide Angle Camera of the Lunar Reconnaissance Orbiter (LROC) on September 8, 2010. The photograph, taken from orbit at 90° east longitude, displays the Moon's near side, revealing prominent lunar plains and mountainous regions. The clear demarcation between the near and far sides of the Moon provides valuable insights for studying the geological features of both hemispheres.

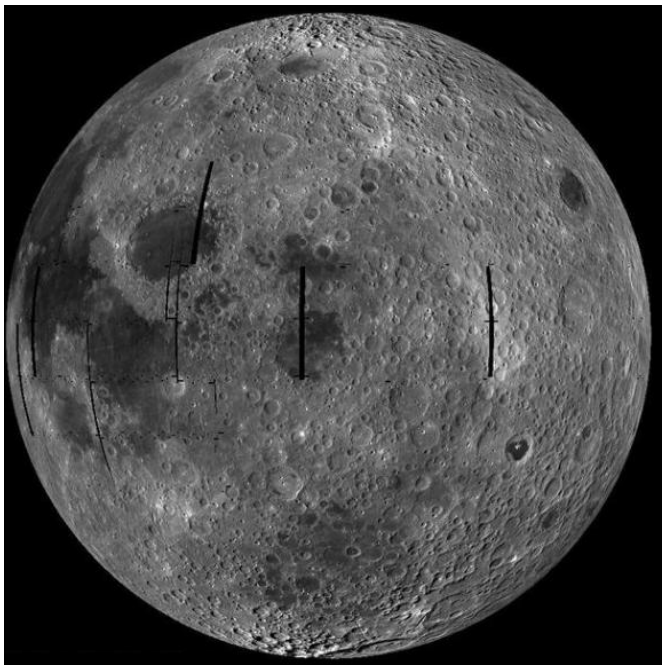

Fig.1. The Moon captured by the Wide Angle Camera of the Lunar Reconnaissance Orbiter (LROC) (*Astronomy, 2023*).

Measurements with the optical location of angular reflectors mounted on the lunar surface, radio interferometry with ultra-long base, and classical terrestrial astrometric observations (photographic, meridian, heliometric, etc.) are used for studying the Moon's dynamic and geometric characteristics. There are more than 30 models of the Moon's gravitational field based on measurements obtained from the Moon's artificial satellites GRAIL, Luna, Explorer, Lunar Orbiter, Apollo spacecraft subsatellites, laser location, ultra-long-range radio interferometry, and measurements of radial accelerations of command and control modules of the Apollo spacecraft (Matsumoto et al., 2010).

An important step in the development of models of the Moon's gravitational field was the launch of the GRAIL mission (Zuber et al., 2013; Goossens et al., 2020), which features two satellites moving one after the other. By measuring the changes in the position of the satellites relative to each other, it was possible to obtain new and more accurate information about the Moon's gravitational field. The mission also provided observation of both the visible side of the Moon and the opposite side. This has led to new and more accurate models of the Moon's gravitational field (Konopliv et al., 2014; Williams et al., 2014). To date, there are several dozen models of the Moon's gravitational field. Before selecting one of these models to address theoretical and practical problems in lunar space and Moon studies, or to interpret results, questions about their reliability arise. There is no doubt that the models constructed cannot be absolutely accurate, because they will always contain measurement errors, as well as errors related to the way the data are processed.

The gravitational field is affected by many parameters, and the most important of them are the parameters of the internal structure (Newton, 1687).

The topography of the Moon is not studied enough. In recent years, there has been a breakthrough in the study of the Moon's topography and its gravitational field, which indicates the beginning of human exploration of space for practical purposes. New models of gravity and height anomalies of the Moon were created. It was caused by numerous missions, which were implemented in various space projects and experiments.

There are also models of the Moon's gravitational field, which can be used to determine certain functionals of this field. However, the resolution of the calculated functionals depends on the order and degree of the original model.

Goal

This paper aims to analyze the development of models of the Moon's gravitational field by selecting one of the models for the relevant time interval of the study of the Moon. To compare them and show the difference with already existing models, as well as to summarize and structure the information about the studied models of the gravitational field of the Moon. Formulate recommendations for the use of these models in future studies.

Research methodology

The input data for the study were obtained with the help of the International Centre for Gravitational Field Models (Ince et al., 2019). Two gravitational field functionals were used in the study: the gravity anomaly and the height anomaly. The input data were placed on a regular 6′×6′ grid. Such a resolution was decided to use for two reasons. First, all figures should have the same resolution. It is crucial for visual comparison, as used in the article, to expose the features of a certain model. It also provides the ability to view the actual data resolution used during model construction. Additionally, it helps to distinguish between different data sets used to construct the model. It will be shown in the next chapters where differences of models are presented (data with real low resolution presented with a smooth surface, that effect can be seen in Figure 15). The second reason is that models with the highest resolution have a degree of approximately 2000 (with some models having more and others less), which corresponds to a grid resolution of 6′×6′ according to the Nyquist rule (model resolution = 180 / model's degree). In future works, more precise statistical techniques are planned to be used. The functional differences of the studied models were plotted for comparative analysis. Data visualization and processing were performed using the GMT software package (Wessel et al., 2013). The final analysis of the models was carried out by comparing and examining the constructed maps of two geopotential functionals, as well as their differences. A similar methodological approach has been adopted in previous studies. For example, Zuber et al. (2013) applied geopotential functionals and satellite-derived gravity data to analyze the structure of the lunar gravity field using GRAIL observations. Likewise, Bucha et al. (2019) used a spherical harmonic framework and topographic constraints to develop high-resolution lunar gravity field models, processed and visualized with GMT. These studies demonstrate the effectiveness of such techniques in the context of lunar geophysics and validate the approach used in this paper.

After a brief description of the overall methodology, let's take a closer look at geopotential functionals that were used in this article. As is well known, the gravitational (attractive) potential is often represented by the harmonic coefficients of the geopotential expansion in a series of spherical functions:

$$V(r,\lambda,\phi) = \frac{GM}{R}\sum_{n=0}^{N_{max}}\sum^{n+1}\sum_{m=0}^{n}\left(\overline{C}_{nm}\,cos(m\lambda) + \overline{S}_{nm}\,sin(m\lambda)\right)\overline{P}_{nm}\,sin\,\phi\left(\frac{R}{r}\right), \quad (1)$$

where:

r,λ,φ - the spatial spherical coordinates: radius, longitude, and latitude, respectively;

GM - the geocentric gravitational constant;

R - the Earth's radius;

$\overline{C}_{nm}, \overline{S}_{nm}$ - the fully normalized spherical harmonic coefficients;

$\overline{P}_{nm}(\sin\varphi)$ - the fully normalized associated Legendre functions.

There are many functions of the geopotential; however, two were selected for this study: gravitation (which is the first derivative of the geopotential with respect to the radial vector) and the height anomaly. This choice is motivated by the fact that gravitation, together with the centrifugal part, is often used to compute gravity anomalies, which in turn have wide applications. For example, it can help in determining the internal density of the Earth's outer layers and thus in the exploration of mineral resources. Meanwhile, the height anomaly is an essential component in the establishment of a reference surface for height systems.

Gravitation can be expressed as follows.

$$g(r,\lambda,\phi) = \frac{GM}{R^2}\sum_{n=0}^{N_{max}}\sum^{n+2}\sum_{m=0}^{n}\left(\overline{C}_{nm}\,cos(m\lambda) + \overline{S}_{nm}\,sin(m\lambda)\right)\overline{P}_{nm}\,sin\,\phi\,(n+1)\left(\frac{R}{r}\right), \quad (2)$$

where g - the gravitational acceleration at a given point.

In contrast, the height anomaly (denoted by ζ) represents the distance between two points, P and Q. The first point - P lies on the Earth's surface where the actual geopotential W is measured. The second point, Q, lies on the intersection of the plumb line passing through point P and the surface of the normal geopotential U, whose value is equal to that of the real geopotential at point P (Fig. 2).

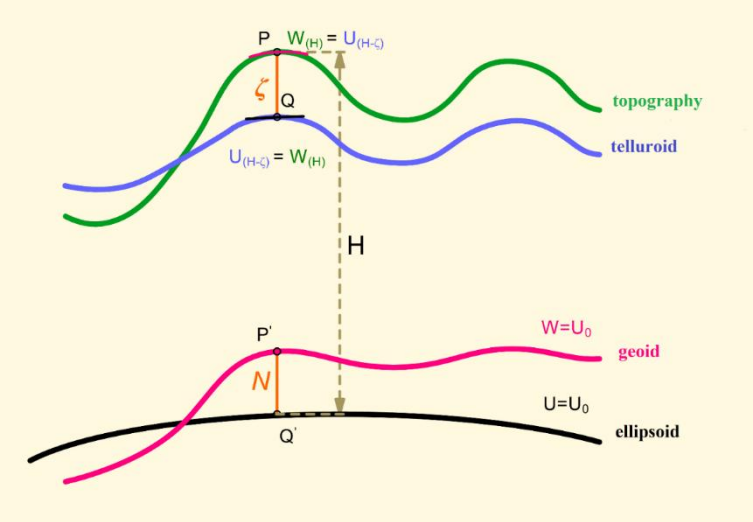

Fig.2. Main reference surfaces in geodesy (Lukianchenko, 2016).

Thus, the height anomaly in the first approximation can be calculated as follows (see ICGEM):

$$\varsigma_{e1}(\lambda,\phi) = \frac{GM}{r_e\gamma(r_e,\phi)}\sum_{n=o}^{N_{max}\Sigma}\left(\frac{R}{r_e}\right)^n \sum_{m=0}^{n} P_{nm}(sin\,\phi)(C_{nm}^{T}\,cos\,m\,\lambda + S_{nm}^{T}\,sin\,m\,\lambda), \quad (3)$$

this can be further refined as:

$$\tilde{\zeta}_1 = \varsigma_{e1} + \frac{H(\phi,\lambda)+N(\phi,\lambda)}{\gamma(0,\phi)} \cdot \left.\frac{\partial T^C}{\partial r}\right|_{r=r_e}, \quad (4)$$

where:

r_e - the radial distance to a point located on the surface of the reference ellipsoid;

$\gamma(r_e,\varphi)$ - the value of normal gravity at a point on the ellipsoid, specified by latitude φ;

n, m - degree and order of the gravity field model;

$H(\varphi,\lambda)$ - the elevation of the topographic surface (topography) at the point defined by coordinates φ,λ;

$N(\varphi,\lambda)$ - the geoid height at the point defined by coordinates φ,λ;

$\left.\frac{\partial T^C}{\partial r}\right|_{r=r_e}$ - the radial derivative of the disturbing potential at a point on the ellipsoid.

More detailed information can be found at ICGEM (Ince et al., 2019).

Research results

Nowadays, there are many models of the lunar gravitational field, so when using these models to solve theoretical and practical problems arising in lunar and lunar space research, questions arise about their reliability in interpreting the results. Of course, an established model cannot be absolutely accurate, since errors in the methods of measurement and processing of results always exist. One important feature that affects the gravitational field is the characteristics of the internal structure of the celestial body.

*T*o obtain a qualitatively consistent gravimetric map of the Moon, tracking results from the Lunar Orbiter mission were taken into account. The results demonstrated that large concentrations of mass extend beneath the lunar rings, called mascons, discovered by Muller & Sjogren (1968) from observations from five Lunar Orbiter spacecraft (USA), and have different significant implications for theories concerning lunar history. The mascons (Barenbaum & Shpekin, 2018) are characterized by significant positive gravity anomalies coinciding with the centers of large lunar basins. Recent studies have refined our understanding of the structure and origin of mascons through high-resolution satellite gravity modelling. Andrews-Hanna et al. (2014) demonstrated that mascons are formed by a combination of impact-induced crustal thinning, volcanic infill, and isostatic adjustment. Zhao et al. (2021) employed three-dimensional gravity inversion of GRAIL data to show evidence of high-density mantle uplift beneath mascon basins, surrounded by low-density crustal rings extending to the lunar Moho. McArdle & Russell (2023) developed high-resolution global point-mascon models, improving the spatial representation of

mascons and providing a refined basis for lunar gravity field modelling. These results confirm the complexity of mascon formation and support the use of modern models for accurate interpretation of the Moon's internal structure and gravity field.

The value of the free-fall acceleration for the Earth is $g = 9.822$ m/s^2, while for the Moon this value is about six times smaller, equal to $g = 1.625$ m/s^2 (Blick et al., 2018).

Although a large volume of models of the gravitational field of the Moon has now been developed, the resolution of the calculated functionals obtained from these models depends directly on the order and degree of the model itself. Therefore, it has become necessary to analyze and compare new modern models of the Moon's gravitational field with earlier and older models.

Five models of the gravitational field of the Moon were chosen for the study (Tab.1).

Tab.1. Moon's gravitational field models.

N	Model name	Year of creation	Order	Data
1	AIUB GRAILV-VGRL 350A	2021	350	GRAIL
2	STU_MoonTopo720_plusNormalField	2019	2160	Topography
3	GRGM660PRIM	2013	660	
4	JGL150Q1	2000	150	
5	GLGM-2	1995	70	

The following algorithm was used to obtain model data:

Go to the ICGEM website (Ince et. al., 2019), then you need to go to the "Calculation Service" tab and configure the following parameters:

- choose the model of the celestial body - the Moon;
- choose the model of the gravitational field of the Moon;
- choose the functional (height anomaly and gravitation);
- set the area of the regular grid.

After the calculation, load the constructed grid file (Fig. 3).

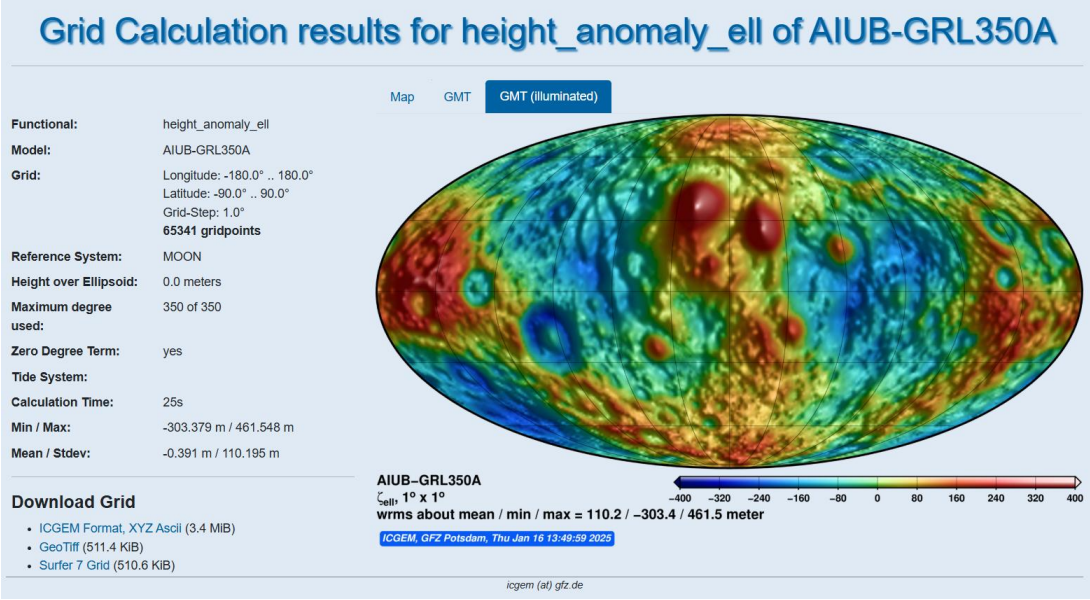

Fig.3. Example of the page International Centre for Global Earth Models (ICGEM), where we can download the calculated grid. (International Centre for Global Earth Models. 2023)

The study was conducted for the entire territory of the Moon. A common amount of 65,341 values for both gravitation and height anomaly was obtained for each model. The data are located on a regular grid with a step size of 1 degree (interpolated on a 6x6 minute grid during data processing).

Two functionals were calculated. Maps of the calculated functional differences were constructed. Comparative analysis of the models was performed. Files with differences of height anomalies and gravity anomalies were created. The file has the following structure: the first column presents latitude, the second presents longitude, and the third presents functional difference. Those files were prepared for each model of the Moon's gravitational field.

Five models of the Moon's gravitational field were selected for the study (Tab.1). The functional differences were calculated for each pair of these models. A total of 20 files with differences were calculated for each of the two geopotential functions (height anomaly and gravity anomaly).

To create maps of the Moon's gravitational field models, an algorithm was compiled, and maps were built using the GMT program.

Constructing maps of the Moon's gravitational field models.

The topographic study of the Moon is not uniform. The most complete and accurate information available today concerns the lunar surface topography of the visible side of the Moon, and the least accurate information is about the far side (Zuber et al., 2013). There are several models that describe the topographic surface of the Moon; one of these is the STU_MoonTopo720_plus Normal Field (Bucha et al., 2019) (Fig. 4), which is represented to degree and order 2160. Today, this model has one of the best resolution capabilities. As can be seen from Fig. 4, the altitudes of the middle near-side of the Moon are on average 3500 m lower than the far-side altitudes.

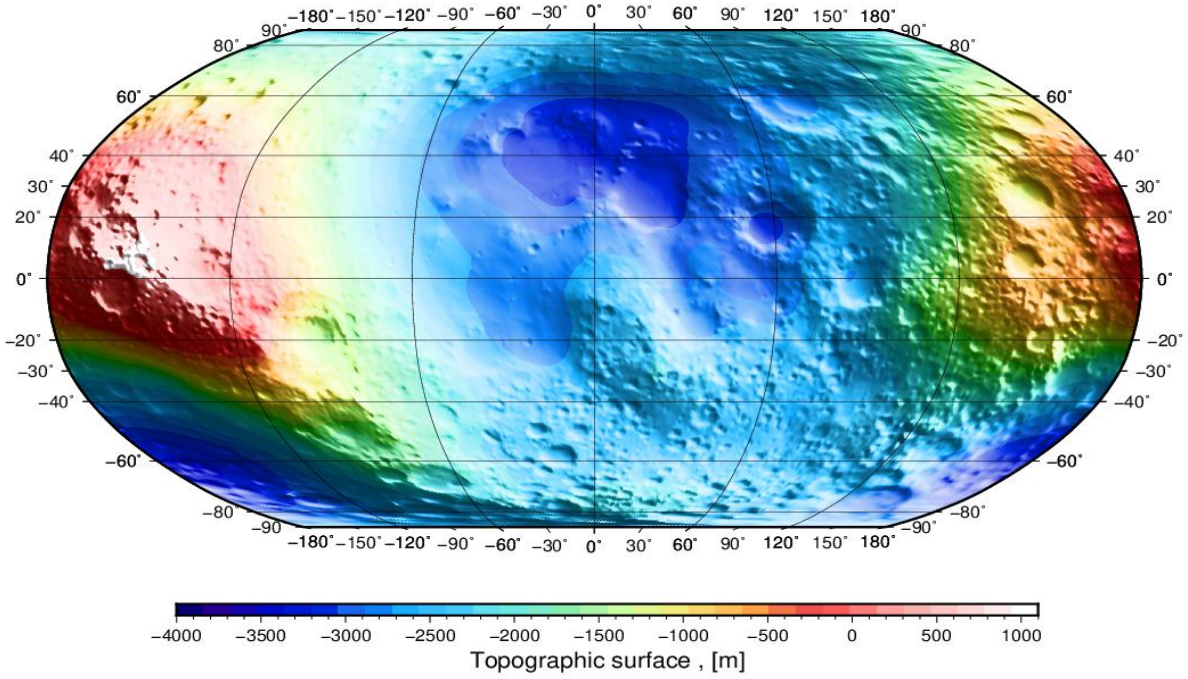

Fig.4. Map of the Moon's topographic surface based on the STU_MoonTopo720_plusNormalField model.

Based on the created grid files, the GMT program was used to build a graphical representation of height anomalies, gravity anomalies, and differences for models of the Moon's gravitational field.

Model 1. AIUB GRAILV-VGRL 350A (Bertone et al., 2021).

This is one of the latest *M*oon's gravitational field models from the GRAIL spacecraft. This model is represented to the 350th degree and order.

Having analyzed the height anomaly map, Fig. 5 clearly shows that the magnitudes of the anomaly take on maximum and minimum values at the locations of lunar mountains and oceans.

At the location of the Tycho Crater (Fig. 5), the height anomaly differs from the surrounding area and acquires values of about 200 - 250 m, and in the area bounding the crater, it is -100 to 0 m. The gravitation at the Tycho Crater location appears to be around 162,300 to 162,700 mGal from the resulting Fig. 4.

To the west of the Tycho crater is crater 2, for which the height anomaly values are significantly less than the surrounding area and range from -200 to -300m, while the area bounded by the height anomaly values range*s* from -100 to 0m. The gravitation for this crater ranges from 161,800 to 162,000 mGal.

The maps (Figs. 5 - 6) show areas where systematic deviations can be seen, which can be caused by the data set obtained for a given area.

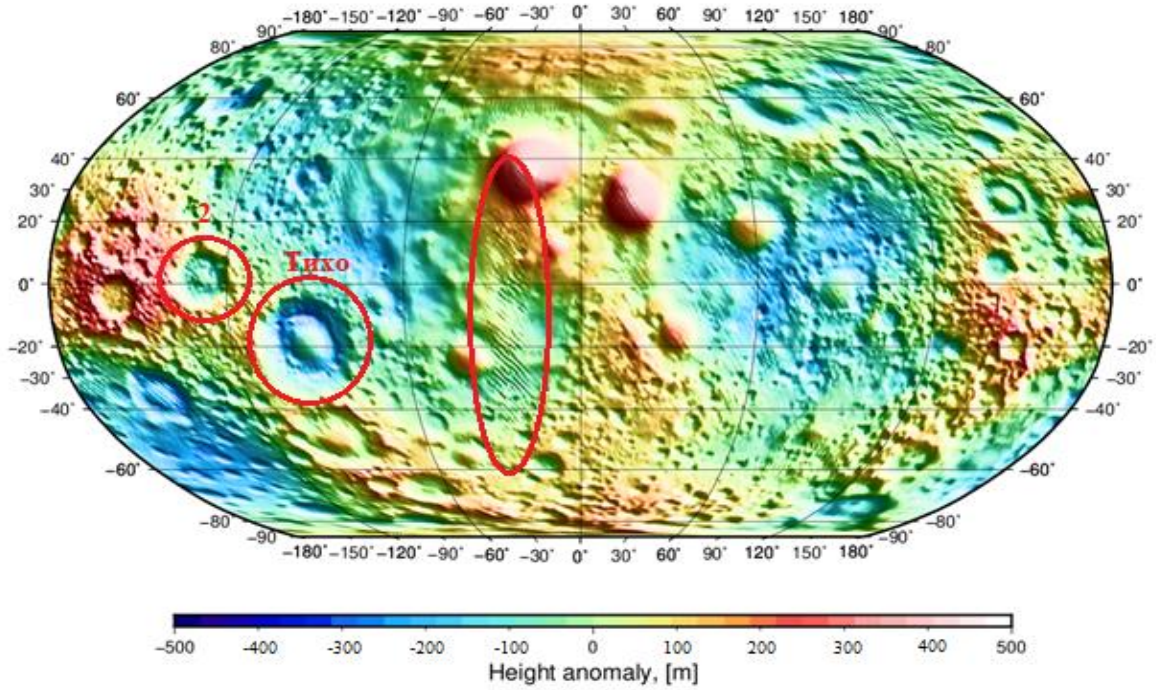

Fig.5. Height anomaly distribution map for the AIUB GRAILV-VGRL 350A model.

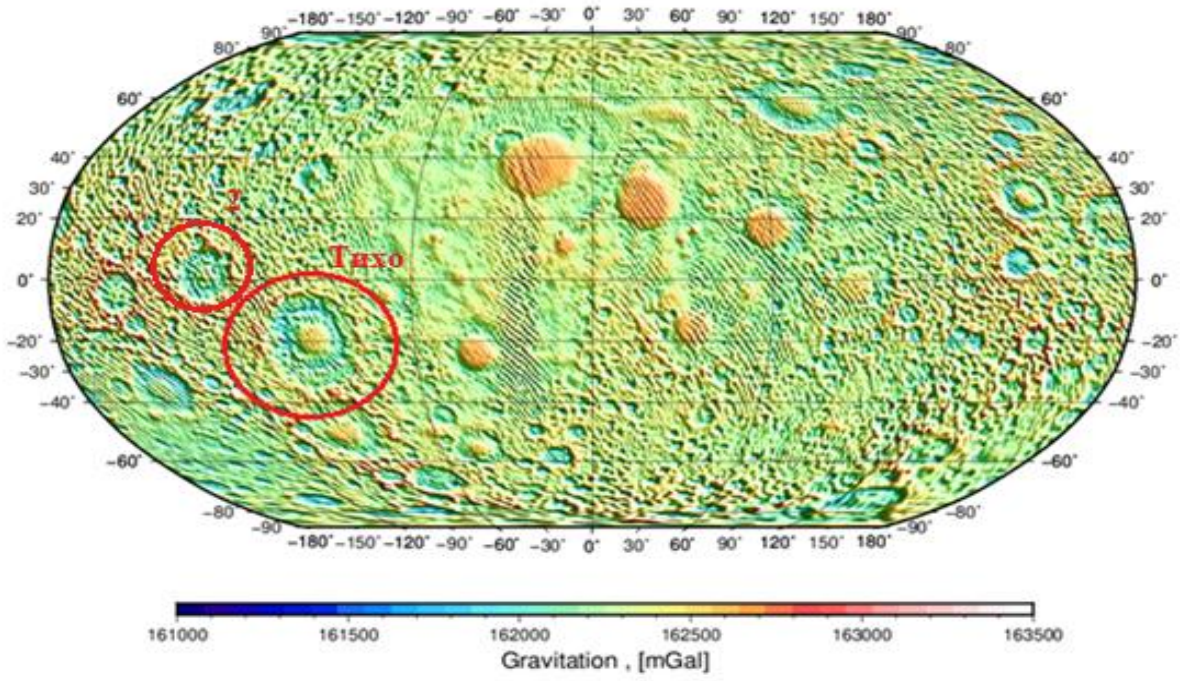

Fig.6. Map of the gravitation distribution for the AIUB GRAILV-VGRL 350A model.

Model 2. GRGM660PRIM (2013), (Fang et al., 2018).

A model of the gravitational field of the Moon is presented to degree and order 660. The map (Fig. 7) shows that the maximum and minimum height anomaly values are at the mascon locations, acquiring values of -459.747 m and -303.075 m, respectively.

The maps (Figs. 7 - 8) clearly show the positions of the lunar seas in the centre of the visible part of the Moon in its northern part because the gravitational force here is different from the general trend and ranges from 162,500

to 162,700 mGal, and for the surrounding area it ranges from 162,100 to 162,300 mGal. Characteristic values of gravitational force for the far part of the Moon are from 161,800 to 163,000 mGal.

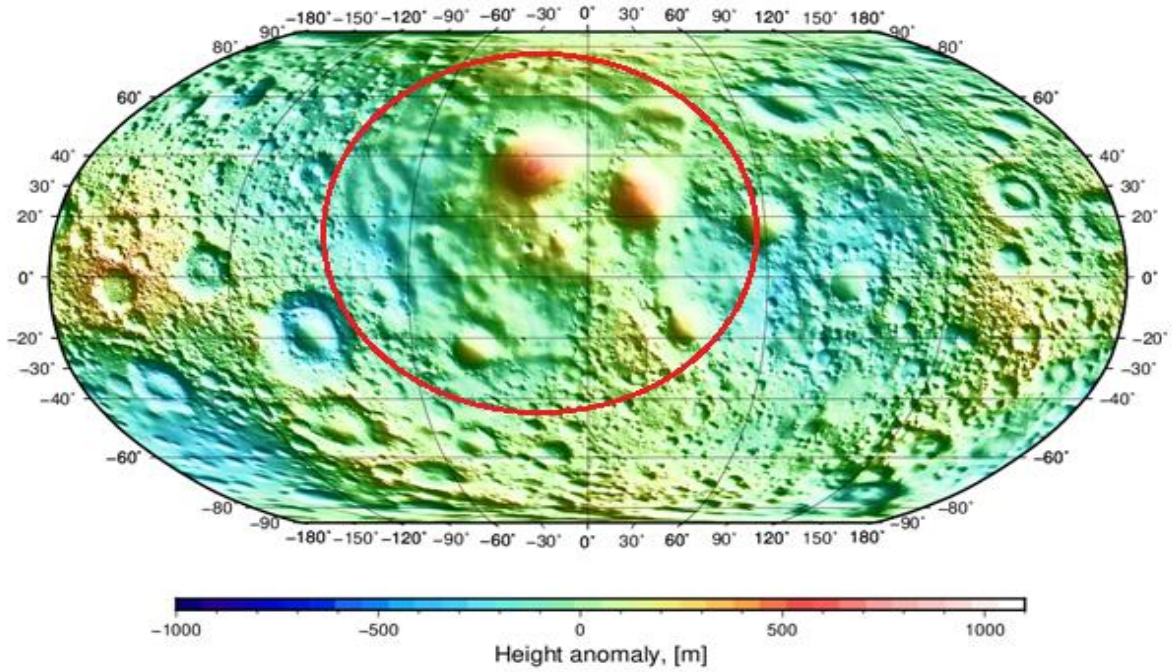

Fig.7. Map of height anomaly distribution for model GRGM660PRIM.

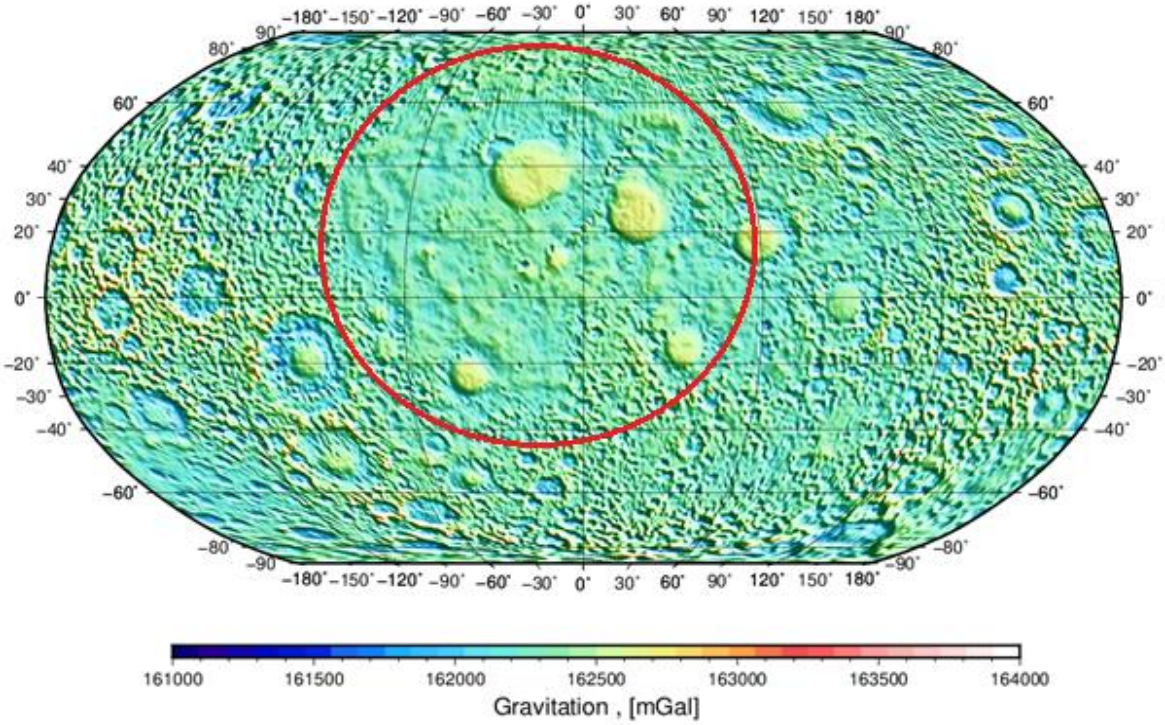

Fig.8. Gravitation distribution map for model GRGM660PRIM.

Model 3. JGL150Q1 (2000)

Model JGL150Q1 (2000) of the gravitational field of the Moon is represented to degree and order 150. The map (Fig. 9) shows that the maximum value is 460.566 m and the minimum value is -295.945 m. Figs. 9 - 10, through satellite traces show the possible influence of the satellite data. But this can also be caused by the method of data processing.

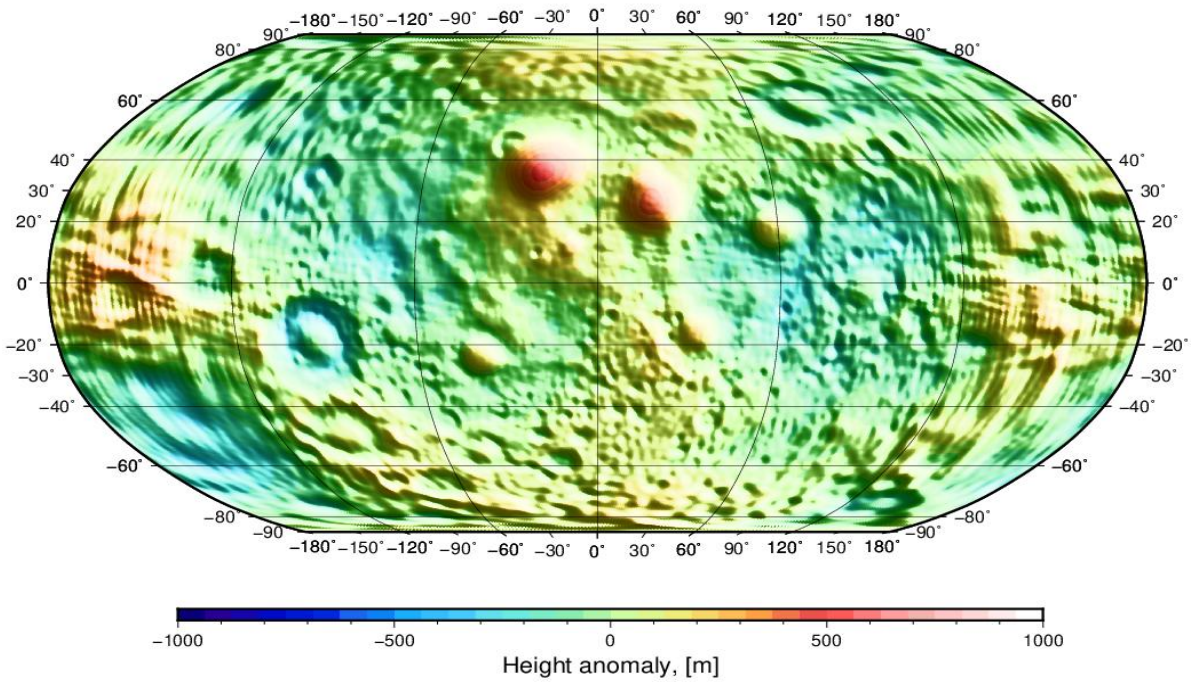

Fig.9. Height anomaly distribution map for model JGL150Q1

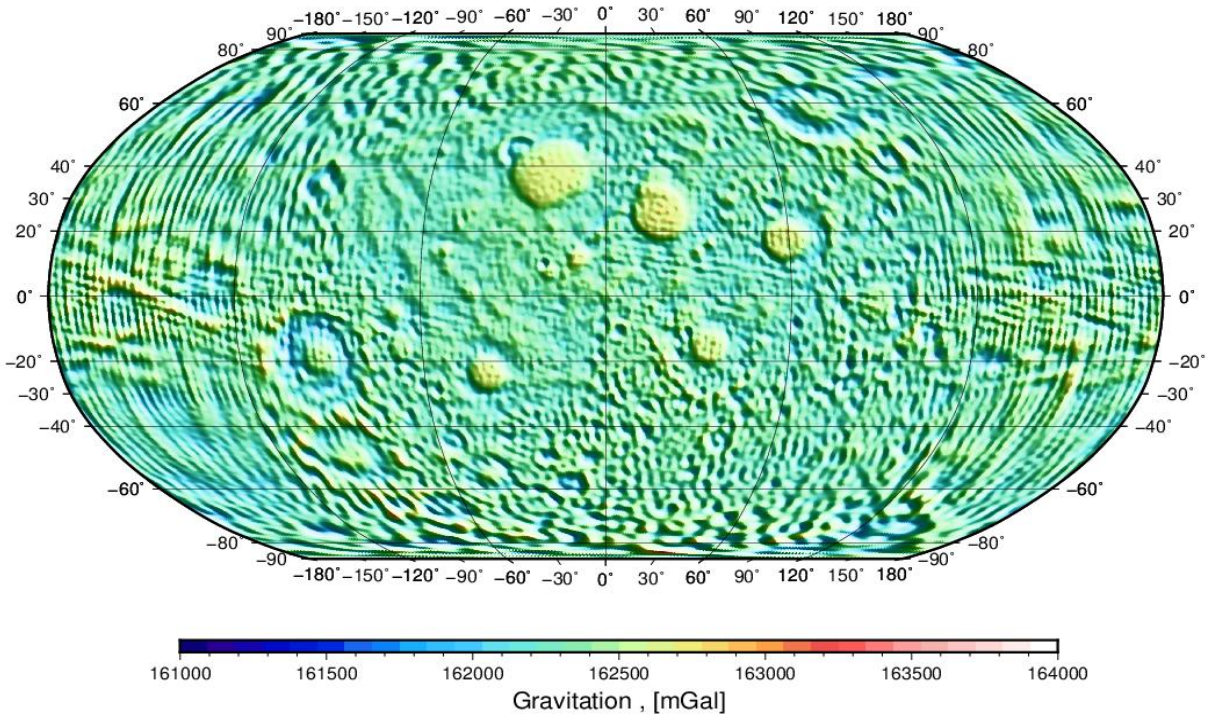

Fig.10. Map of gravitation distribution for model JGL150Q1.

Model 4. GLGM-2 (1995).

The GLGM-2 model of the Moon's gravitational field (Figs. 11-12) is represented to degree and order 70. The low order of the model is due to the year of its creation, as there were insufficient data (in quantity and quality) to construct a higher order model at this time.

For this model, the values of height anomaly vary between -271.905m and 475.067m.

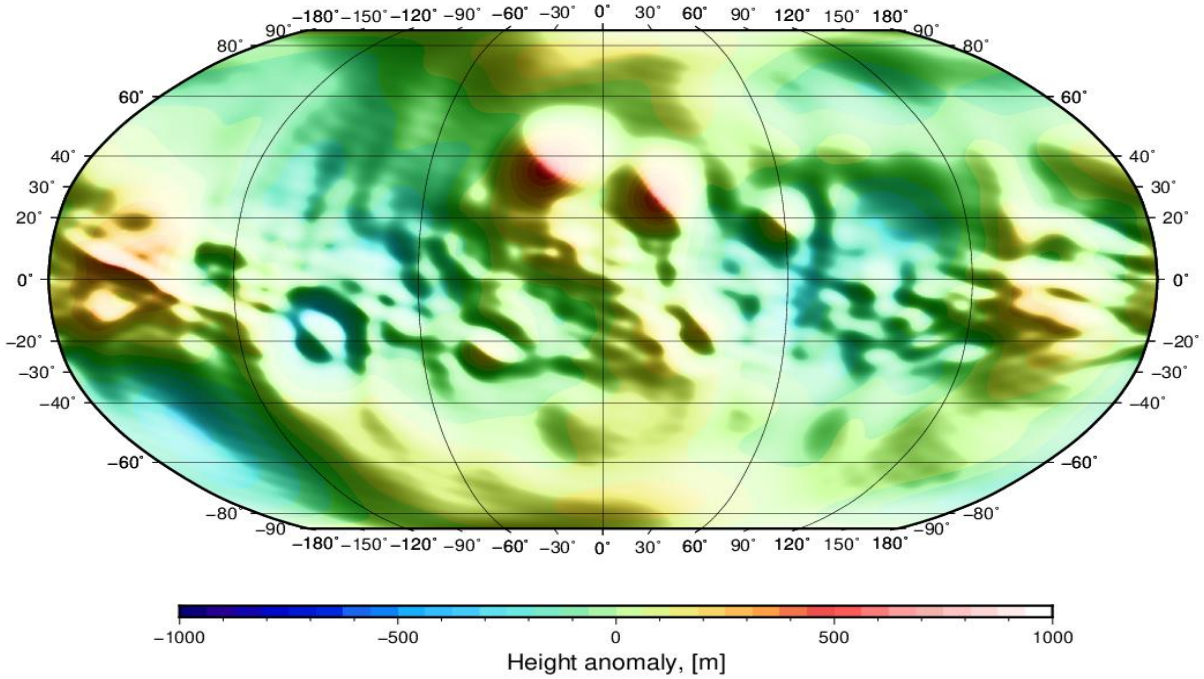

Fig.11. The height anomaly distribution map for model GLGM-2.

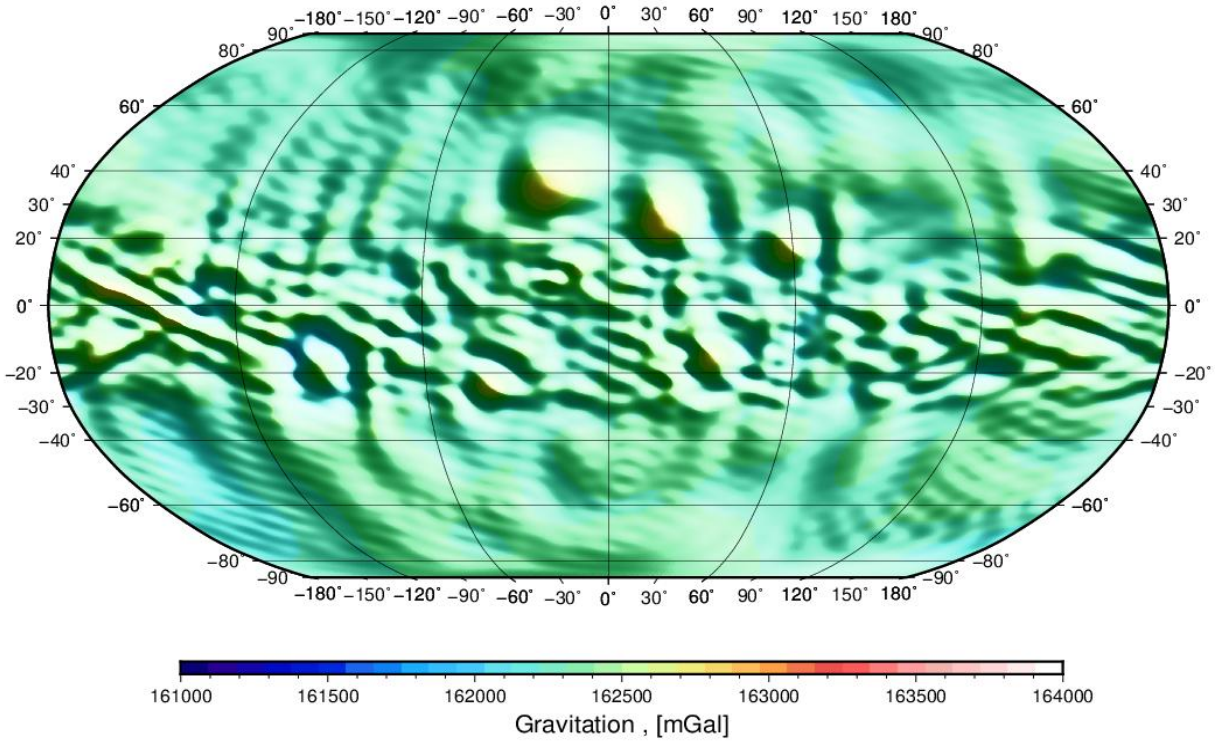

Fig.12. The gravitation distribution map for model GLGM-2.

Mapping for height anomaly differences.

In topographic terms, the Moon is unevenly studied. Currently, the most complete and accurate information about the lunar topography is on the visible side of the Moon, while the least accurate information is on the far side (Tserklevych, 2009). There are several models to describe the Moon's topographic surface, one of them being STU_MoonTopo720_plus Normal Field (Fig. 4), which is represented to degree and order 2160. To date, this

model has the best resolution. As can be seen from the figure, the central part (near side) of the Moon has altitudes on average 3500 m lower than on the far side.

Comparison of models of the gravitational field of the Moon was carried out as follows: the height anomaly differences between two models were determined, and the calculated results were mapped (Figs. 13-16).

Fig. 13 shows the height anomalies between two models of the gravitational field of the Moon, namely between the AIUB model GRAILV-VGRL 350A (2021) and JGL150Q1 (2000). These models are based on the results of the two space missions GRAIL and Lunar Prospector, respectively. The GRAIL mission explored the entire Moon, while the Lunar Prospector mission probably only explored the visible side of the Moon. Therefore, it is evident that the differences in height anomalies are more pronounced at the edges of the maps and less pronounced in the middle.

The height anomaly differences between AIUB GRAILV-VGRL 350A (2021) and GRGM660PRIM (2013) are analyzed:

In the older GRGM660PRIM, the near side was better studied and investigated. When comparing it to the new AIUB GRAILV-VGRL 350A model on the visible side of the Moon, the differences in height anomalies have a uniform distribution over the entire area and are ±1m, indicating mostly approximate values for the models in the study area (Fig. 14).

The far side of the Moon in the older model JGL150Q1 was extrapolated due to a lack of data, so when comparing it to the new one, a significant and irregular difference of ±50m in height anomaly was found (Fig. 14). Similar variations for height anomaly difference are evident between model GRGM660PRIM and JGL150Q1 (Fig. 15).

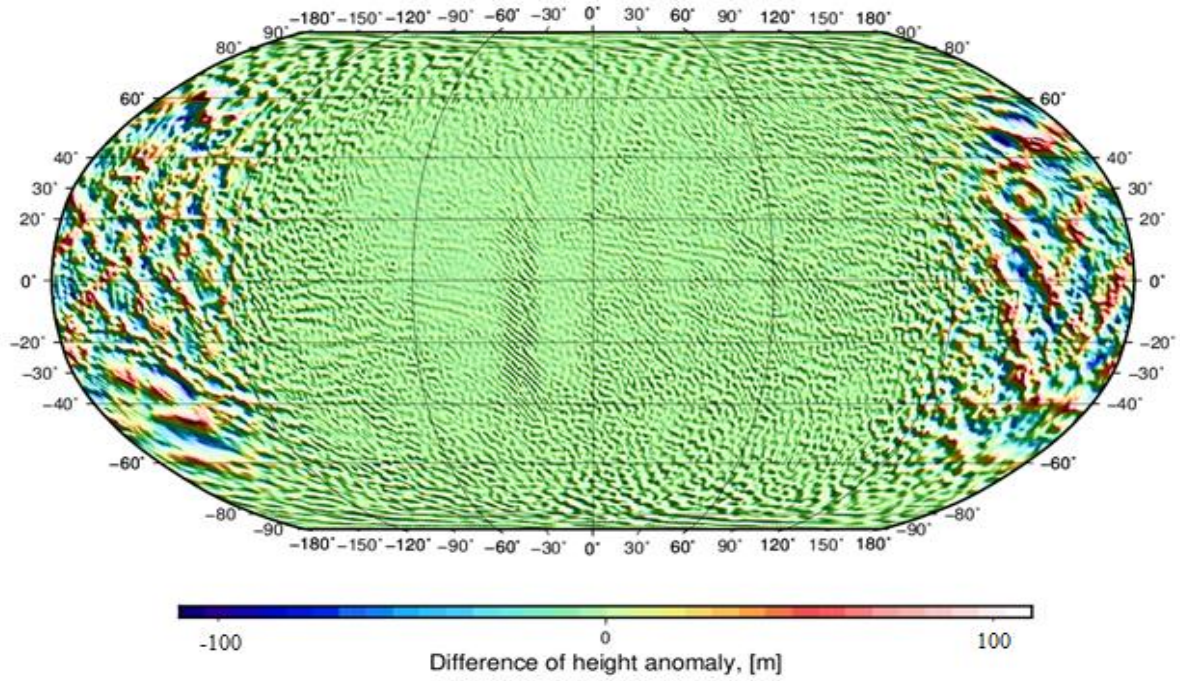

Fig.13. AIUB GRAILV-VGRL 350A and JGL150Q1 height anomaly difference map.

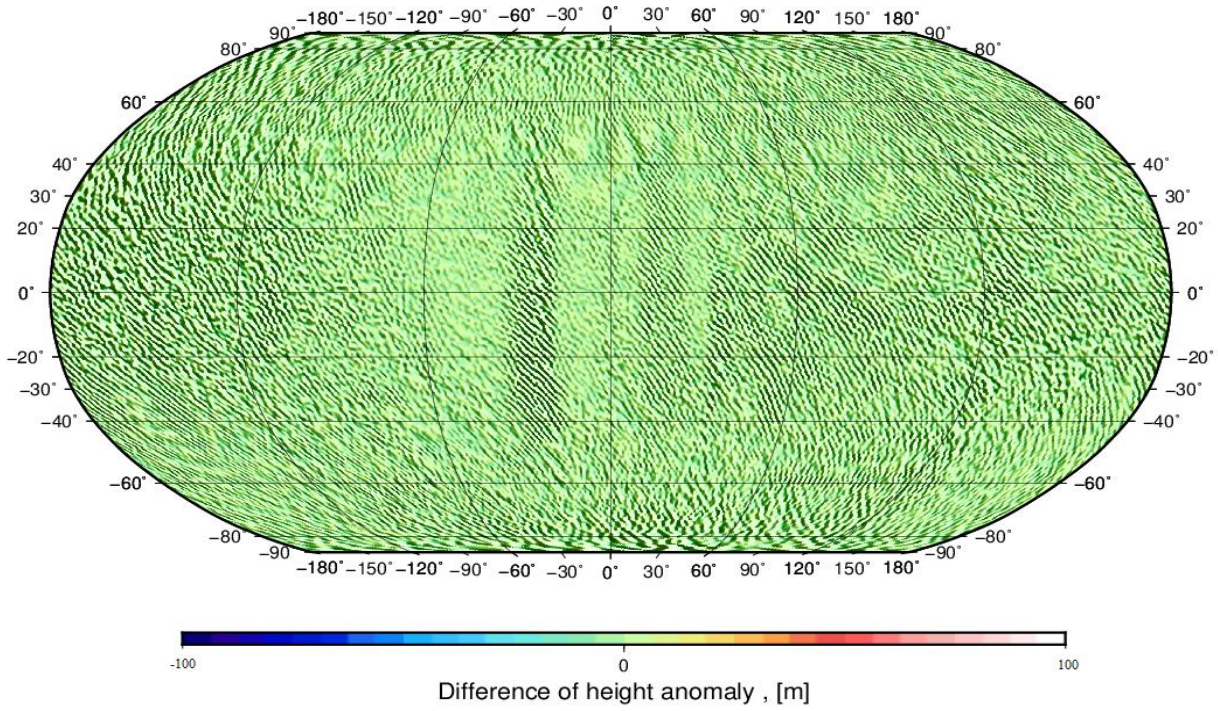

Fig.14 AiuB GRAILV-VGRL 350A and GRGM660PRIM height anomaly difference map.

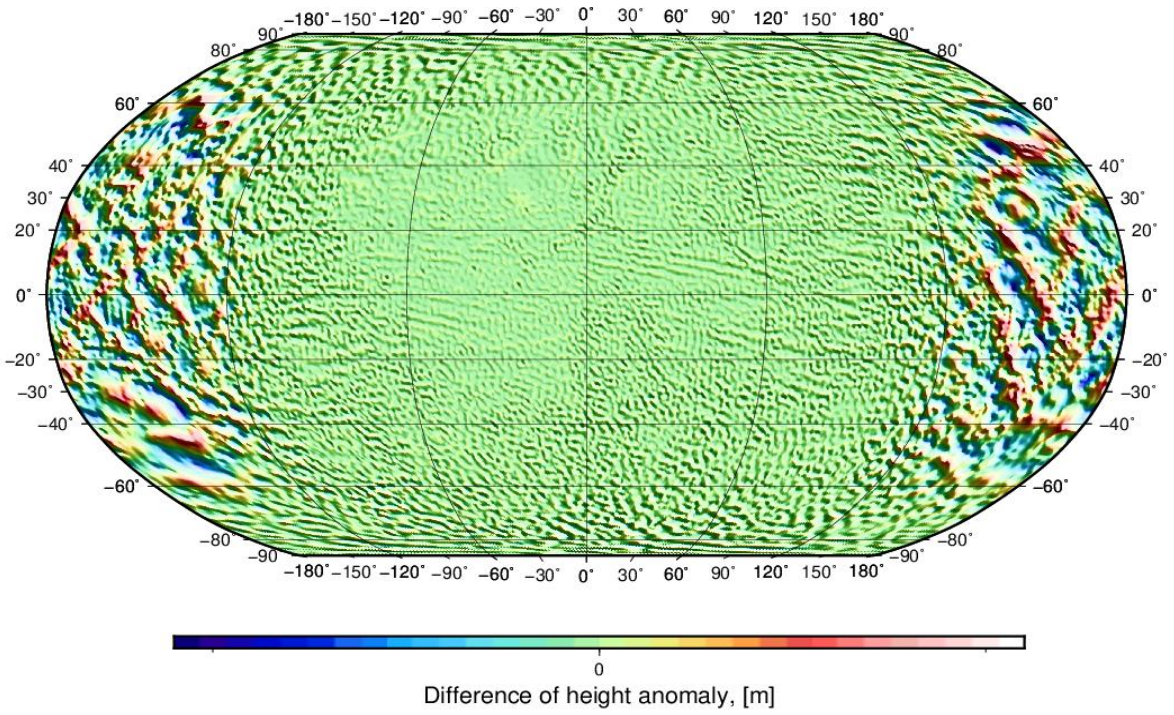

Fig.15. Mapping of height anomaly difference between GRGM660PRIM and JGL150Q1.

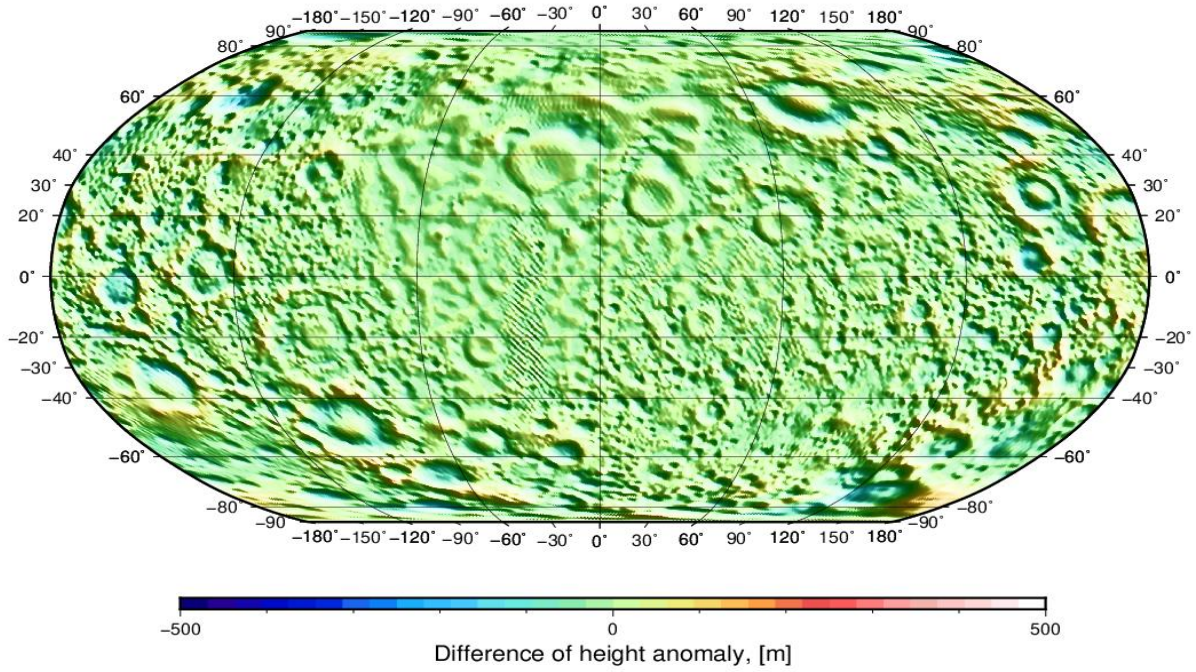

Fig.16. Map of differences of height anomalies of AIUB GRAILV-VGRL 350A and GLGM-2.

Mapping for gravitation differences.

An algorithm for comparing the gravity of lunar gravitational field models is developed similarly to that for height anomaly differences. Fig. 17 shows the difference in gravitation between the two AIUB models GRAILV-VGRL 350A (2021) and GLGM-2 (1995). The influence of satellite data at latitudes from -40 to -90 degrees is shown in Fig. 16. It is likely that data from other satellites were used, which caused such a drastic change. One more thing should be noticed here. When discussing gravity, we take centrifugal force into account; however, in the case of gravitation, we consider the Moon as a static object without centrifugal force. When differences of gravitation are obtained, they are equivalent to differences of gravity, as centrifugal force is absent in both cases. That is why the next figures are called “gravity differences”.

The difference in gravitation between the AIUB GRAILV-VGRL 350A and GRGM660PRIM models is shown in Fig.18. One of the models is more accurate, so relief features are apparent. The figure illustrates the potential impact of satellite data of comparable order and accuracy, represented by satellite traces at -40 parallels.

Fig.18 clearly shows the location of the plains on the Moon, the so-called lunar seas, located on the near side of the Moon in its central-northern part, as the gravitation here differs from the general trend and ranges from 162,500 to 162,700 mGal.

The difference in the gravitation of GLGM-2 and GRGM660PRIM is shown in Fig. 19. Here, we can see a flat area in the central part clearly reflecting the position of the lunar seas on the near side of the Moon. It is known that impact craters are more concentrated on the back side of the Moon, so the figure clearly demonstrates where the side is more battered by meteorites.

Other maps of the functional differences have also been constructed, clearly showing the features of the studied Moon's gravitational field models, which, although not presented here, are also analyzed.

When studying the lunar gravitational field, certain functionals are used; specifically, the height anomaly and gravity are used in this paper.

We have created maps of gravitation and height anomalies.

On some maps of gravitational difference, the influence of satellite data is noticeable at latitudes from -40 to -90 degrees. It is possible that data from another satellite was used, which could have caused such a drastic transition.

The created difference maps for the studied functionals demonstrated the features of comparative models.

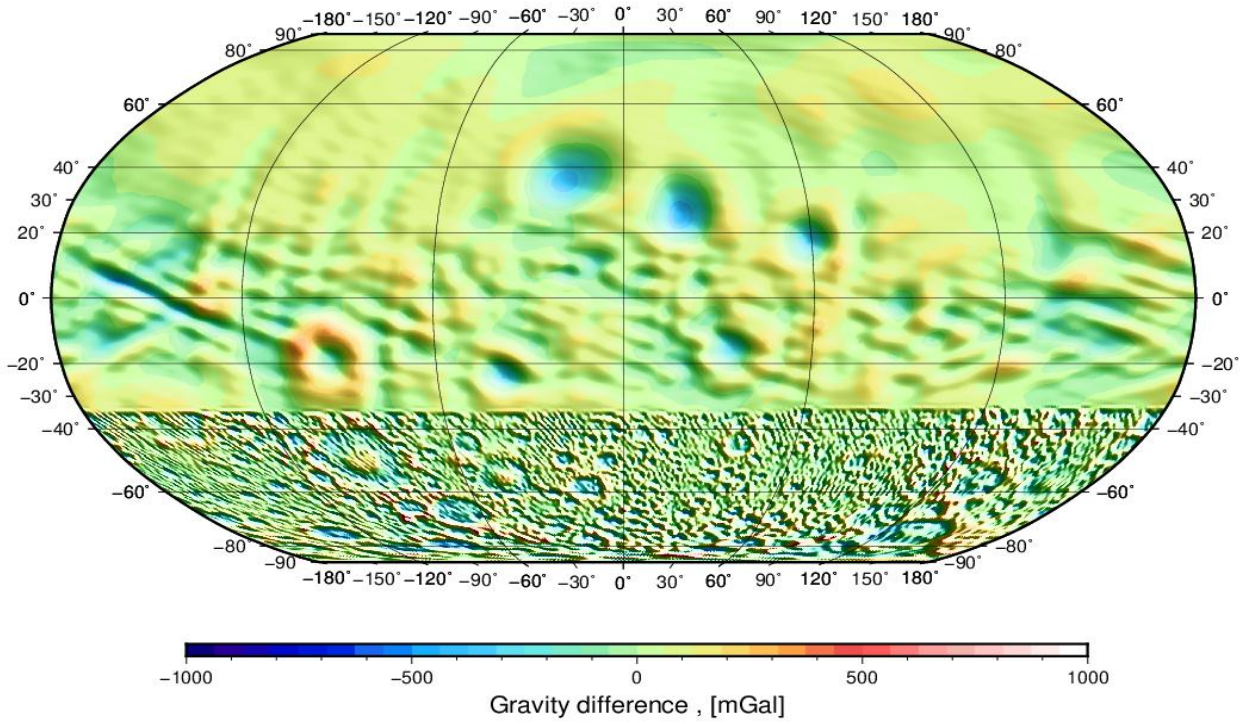

Fig.17. AIUB GRAILV-VGRL 350A and GLGM-2 gravity difference mapping (below figure).

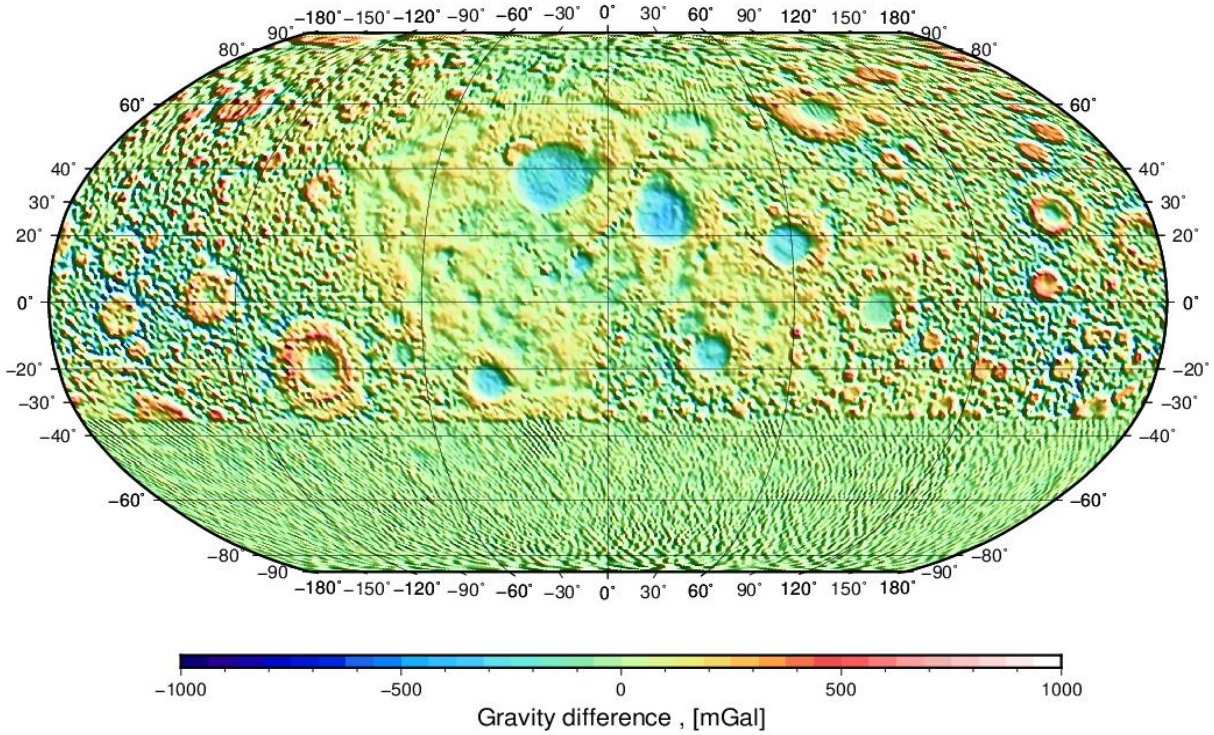

Fig.18 AIUB GRAILV-VGRL 350A and GRGM660PRIM gravity difference mapping.

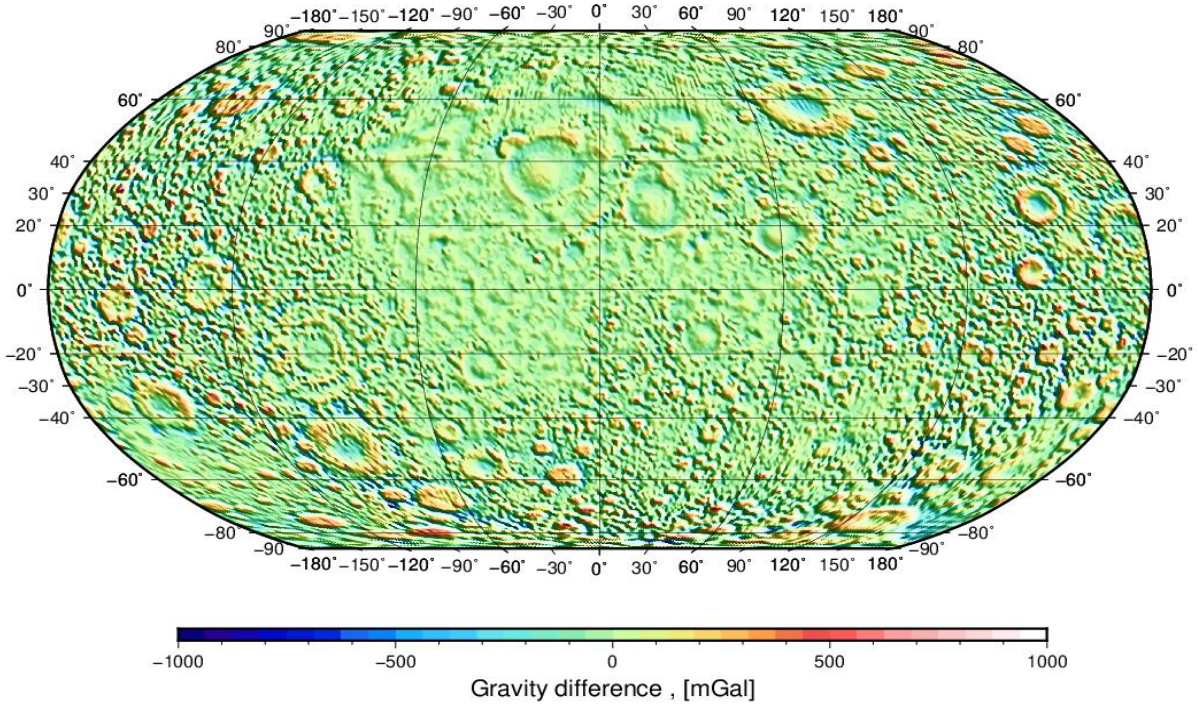

Fig.19. The map of the gravitation differences GLGM-2 and GRGM660PRIM.

Scientific novelty and practical significance

Exploration of our planet has always had top priority, but with the development of space technology and mass launches of spacecraft, interest in other celestial bodies is only increasing.

In recent years, research into the Moon's topography and gravitational field has developed rapidly, signalling the beginning of human exploration of space for practical purposes. Many missions undertaken by various space projects and experiments have resulted in numerous new models of the Moon's gravitational and height anomalies. From such models, certain functionals of the gravitational field can be calculated. However, the resolution of the functionals calculated with these models directly depends on the order and degree of the model itself.

The Moon is the closest celestial body to us and is regarded as an intermediate station for access to space, which makes the study of the Moon's gravitational field particularly relevant. There are already a number of state-of-the-art models of the Moon's gravitational field based on current satellite missions. By summarizing the information on the new models, scientists will be able to understand the features of a particular model better. This will enable a faster and better model selection for a particular study by other scientists, which will facilitate further development and new research. Moreover, this study demonstrates that different lunar gravity models can represent various regions of the Moon’s surface with varying levels of accuracy. For example, the far side of the Moon tends to be modeled with lower precision, as seen in the case of the JGL150Q1 model. In contrast, the GLGM-2 model provides relatively high accuracy in the equatorial regions, while the polar areas are characterized by significantly poorer data resolution. These spatial variations in model accuracy should be carefully considered when developing new models of the Moon’s gravity field. From a practical perspective, this study can be viewed as a comparative assessment of the strengths and limitations of existing gravity models, offering valuable guidance for researchers selecting a model for specific applications. Furthermore, the identified deficiencies should be addressed in the development of future lunar gravity field models.

Conclusions

The current state of the study of the Moon's topography and gravitational field has been investigated. The topography of the Moon is unevenly studied. The most complete and accurate information is available for the visible side of the Moon. As a result, it is determined that the STU_MoonTopo720_plusNormalField (2019) model is the most informative for describing the topographic surface of the Moon, which also has the best resolution (5' x 5', 2160 degrees).

From the constructed and analyzed maps, the gravitation and height anomalies are determined:

- the locations of the lunar mountains and oceans exhibit extreme values of height anomalies;

- the value of gravitation on the Moon ranges from 162 Gal to 163 Gal, with the highest values at locations of lunar seas;
- for JGL150Q1, a possible influence of satellite data was detected, as indicated by the satellite traces in the plotted maps. This effect is also possible through data processing. This has to be taken into account when using the model. In order to smooth the built transforms, we recommend using data filtering;
- the GLGM-2 model is represented to degree and order 70. As the model is based on data from 1995 (at that time, there were not enough data to build a higher-order model), it is of low degree and order.

Functional difference maps are constructed, where the features of the models compared are clearly visible.

As the older models have better studied and explored the near side, when compared with the new models, the near-Earth side of the Moon has defined differences in height anomalies of a gentle, uniform distribution over the entire area. (unclear sentence) This indicates well-correlated values for the models compared. And because the far side was extrapolated due to a lack of data, significant and unequal height anomaly differences appear when comparing it to the new model.

The plotted difference maps for certain functionals illustrated the features of the comparison models. Following a detailed analysis of height anomalies and gravitation maps, it was determined that the lunar gravitational field models from the latest missions (newer) - AIUB GRAILV-VGRL 350A (2021) and GRGM660PRIM (2013) are more informative and suitable for use.

References

Andrews-Hanna, J. C., Asmar, S. W., Head, J. W., Kiefer, W. S., Konopliv, A. S., Lemoine, F. G., & Zuber, M. T. (2014). Structure and evolution of the lunar Procellarum region as revealed by GRAIL gravity data. Nature, 514(7520), 68–71. https://doi.org/10.1038/nature13697

Astronomy. (2023). https://www.astronomy.com/space-exploration/nasas-lunar-spacecraft-completes-exploration-mission-phase/

Barenbaum, A. A., & Shpekin, M. I. (2018). Problem of lunar mascons: An alternative approach. Journal of Physics Conference Series, 2018, vol. 946, no. 1. doi:10.1088/1742-6596/946/1/012079

Bertone, S., Arnold, D., Girardin, V., Lasser, M., Meyer, U., & Jäggi, A. (2021). Assessing reduced Bertone - dynamic parametrizations for GRAIL orbit determination and the recovery of independent lunar gravity field solutions. Earth and Space Science, 8, e2020EA001454. https://doi.org/10.1029/2020EA001454

Blick, C., Freeden, W., & Nutz, H. (2018). Gravimetry and exploration. In Handbook of Mathematical Geodesy, pp. 687-751. Birkhäuser, Cham.

Bucha, B., Hirt, C. & Kuhn, M. (2019). Divergence-free spherical harmonic gravity field modelling based on the Runge–Krarup theorem: a case study for the Moon. J Geod 93, 489–513, 2019. https://doi.org/10.1007/s00190-018-1177-4

Fang Yuan, Meng Xiao-hong, Wang Jun, & Chen Zhao-xi. (2018). Study of the characteristics of lunar gravity field based on the model GRGM660PRIM[J]. Progress in Geophysics, 2018, 33(6): 2211-2218. doi: 10.6038/pg2018CC0118

Goossens, S., Sabaka, T.J., Wieczorek, M.A., Neumann, G.A., Mazarico, E., Lemoine, F. G., Nicholas, J. B., Smith, D. E. & Zuber, M. T. (2020). High-Resolution Gravity Field Models from GRAIL Data and Implications for Models of the Density Structure of the Moon's Crust. Journal of Geophysical Research: Planets: Volume 125, Issue 2, 2020. https://doi.org/10.1029/2019JE006086

Ince, E. S., Barthelmes, F., Reißland, S., Elger, K., Förste, C., Flechtner, F., & Schuh, H. (2019). ICGEM – 15 years of successful collection and distribution of global gravitational models, associated services and future plans. - Earth System Science Data, 11, pp. 647-674, doi: http://doi.org/10.5194/essd-11-647-2019

International Centre for Global Earth Models. (2023). https://icgem.gfz-potsdam.de/home

Konopliv, A., Park, R., Yuan D-N., Asmar, S., Watkins, M., Williams, J., Fahnestock, E., Kruizinga, G., Paik, M., Strekalov, D., Harvey, N., Smith, D. & Zuber M. (2014). High-resolution lunar gravity fields from the GRAIL Primary and Extended Missions. Geophysical Research Letters: Volume 41, Issue 5, pages 1452-1458, March 16 2014. https://doi.org/10.1002/2013GL059066

Lukianchenko, Iu. (2016). The application of satellite and ground data for construction of Earth's gravitational field models. Lviv Politechnic National University, p.20. https://www.researchgate.net/publication/313063777_The_application_of_satellite_and_ground_data_for_construction_of_Earth's_gravitational_field_models_Zastosuvanna_suputnikovih_ta_nazemnih_danih_dla_pobudovi_modelej_gravitacijnogo_pola_Zemli

Mc Ardle, S., & Russell, R. P. (2023). High-resolution global point mascon models for the Moon. Journal of Guidance, Control, and Dynamics. https://doi.org/10.2514/1.G006921

Matsumoto, K., Goossens, S., Ishihara, Y., Liu, Q., Kikuchi, F., Iwata, T., Namiki, N., Noda, H., Hanada, H., Kawano, N., Lemoine, F.G., & Rowlands, D.D. (2010). An improved lunar gravity field model from SELENEand historical tracking data: Revealing the farsidegravity features. JOURNAL OF GEOPHYSICAL RESEARCH, 2010, VOL. 115, E06007, doi:10.1029/2009JE003499

Muller, P., & Sjogren,W. (1968). "Mascons: lunar mass concentrations". Science. 161 (3842): 680-684. www.science.org/doi/10.1126/science.161.3842.680

Newton Isaac. (1687). Philosophiae Naturalis Principia Mathematica. London. pp. Theorem XXXI.

Tserklevych, A. (2009). The current state of the study of the gravity field and topography of the terrestrial planets. Scientific journal "Modern achievements of a geodetic science and industry", ukrainian version: Сучасний стан вивчення гравітаційного поля та топографії планет земної групи, (1)17, 2009, 322–332. https://vlp.com.ua/files/53_7.pdf

Wessel, P., Smith, W. H. F., Scharroo, R., Luis, J., & Wobbe, F. (2013). Generic Mapping Tools: Improved Version Released, EOS Trans. AGU, 94(45), p. 409–410, 2013. doi:10.1002/2013EO450001

Williams, J., Konopliv, A., Boggs, D., Park, R., Yuan D-N., Lemoine, F., Goossens, S., Mazarico, E., Nimmo, F., Weber, R., Asmar, S., Melosh, H., Neumann, G., Phillips, R., Smith, D., Solomon, S., Watkins, M., Wieczorek, M., Andrews-Hanna, J., Head, J., Kiefer, W., Matsuyama, I., McGovern, P., Taylor, G.J., & Zuber. M. (2014). Lunar interior properties from the GRAIL mission. (2014). Journal of Geophysical Research: Planets: Volume 119, Issue 7, pages 1546-1578, July 2014. https://doi.org/10.1002/jgre.20134

Zhao, G., Liu, J., Chen, B., & Kaban, M. K. (2021). 3D density structure of the lunar mascon basins revealed by a high-efficient gravity inversion of the GRAIL data. Journal of Geophysical Research: Planets, 126(5), e2021JE006841. https://doi.org/10.1029/2021JE006841

Zuber, M. T., Smith, D. E., Watkins, M. M., Asmar, S. W., Konopliv, A. S., Lemoine, F. G., & Yuan, D. N. (2013). Gravity field of the Moon from the Gravity Recovery and Interior Laboratory (GRAIL) mission. Science, 339(6120), 668–671. https://doi.org/10.1126/science.1231507